Video Article

Pool-Boiling Heat-Transfer Enhancement on Cylindrical Surfaces with Hybrid Wettable Patterns

Sujith Kumar C.S.*[1], Yao Wen Chang*[1], Ping-Hei Chen[1]

[1]Department of Mechanical Engineering, National Taiwan University

*These authors contributed equally

Correspondence to: Ping-Hei Chen at phchen@ntu.edu.tw

URL: https://www.jove.com/video/55387
DOI: doi:10.3791/55387

Keywords: Engineering, Issue 122, Pool boiling, interlines, superhydrophilic, boiling heat-transfer coefficient, pool-boiling curve, bubble dynamics.

Date Published: 4/10/2017

Citation: Kumar C.S., S., Chang, Y.W., Chen, P.H. Pool-Boiling Heat-Transfer Enhancement on Cylindrical Surfaces with Hybrid Wettable Patterns. *J. Vis. Exp.* (122), e55387, doi:10.3791/55387 (2017).

Abstract

In this study, pool-boiling heat-transfer experiments were performed to investigate the effect of the number of interlines and the orientation of the hybrid wettable pattern. Hybrid wettable patterns were produced by coating superhydrophilic SiO_2 on a masked, hydrophobic, cylindrical copper surface. Using de-ionized (DI) water as the working fluid, pool-boiling heat-transfer studies were conducted on the different surface-treated copper cylinders of a 25-mm diameter and a 40-mm length. The experimental results showed that the number of interlines and the orientation of the hybrid wettable pattern influenced the wall superheat and the HTC. By increasing the number of interlines, the HTC was enhanced when compared to the plain surface. Images obtained from the charge-coupled device (CCD) camera indicated that more bubbles formed on the interlines as compared to other parts. The hybrid wettable pattern with the lowermost section being hydrophobic gave the best heat-transfer coefficient (HTC). The experimental results indicated that the bubble dynamics of the surface is an important factor that determines the nucleate boiling.

Video Link

The video component of this article can be found at https://www.jove.com/video/55387/

Introduction

A high heat flux-sustaining system providing cooling in the range of 10-10^5 W/cm^2 is required in the emerging fields of electronics, defense, avionics, and nuclear device development. Conventional cooling with air is insufficient for these applications due to the low heat-transfer coefficient (HTC) for both free- and forced-convection conditions. The phase change-based cooling techniques, such as pool boiling and flow boiling, are good enough to remove high heat fluxes on the order of 10 - 1,000 W/cm^2 [1]. Since the two-phase heat-transfer process is isothermal, the cooled device temperature is almost constant over its surface. Due to the negligible variation of the temperature along the surface, the thermal shock of the device can be eliminated. However, the major limiting parameter in boiling heat-transfer is the critical heat flux (CHF), which causes an abnormal rise in temperature[2].

In the last few decades, extensive research has been carried out to improve the CHF by using surface modification, nanofluids, and surface coatings[3,4,5,6,7,8,9,10,11]. Among the various methods, surface coatings are found to be the best method to improve the CHF due to the substantial increase in the surface area. Surface coatings generally increase the heat transfer by fin action, porosity effects, and surface wettability[12]. Surface wettability plays a significant role in boiling heat-transfer. Previous studies show that at lower heat-flux conditions, the hydrophobic surface shows better HTC due to the early nucleation. However, at higher heat flux, the detachment of the formed bubbles is slow due to the low affinity of water towards the surface. This leads to bubble coalescence and results in a lower CHF[3]. On the other hand, a hydrophilic surface produces a higher CHF, because of the fast detachment of the formed bubbles, but it gives a lower HTC at low heat fluxes, due to the delay in bubble nucleation[13].

The hybrid structures show a remarkable enhancement in boiling heat-transfer for all heat fluxes due to the combined effect of hydrophobicity and hydrophilicity[14,15,16]. Hsu *et al.* produced heterogeneous wettable surface by coating superhydrophilic Si nanoparticles on a masked copper surface. They achieved different wettability ratios by varying the coating time. The onset of boiling occurred earlier on the heterogeneous surfaces compared to the homogeneous surface, which substantially reduced the wall superheat[17]. Jo *et al.* conducted nucleate boiling heat-transfer studies on hydrophilic, hydrophobic, and heterogeneous wetting surfaces. The heterogeneous wetting surface was composed of hydrophobic patterned dots on the hydrophilic surface. They got higher HTCs and the same CHF for the heterogeneous surface as compared to the hydrophilic surface. An improvement in boiling heat-transfer directly depends upon the number of dots on the surface and upon the boiling conditions[18].

In this study, axial hybrid wettable patterns were produced on a cylindrical copper surface using the dip coating technique. Pool-boiling heat-transfer studies were conducted to determine the effects of the number of interlines and of the orientation of the hybrid wettable pattern. Boiling heat flux, HTC, and bubble dynamics were analyzed for the all coated substrates and were compared with the copper substrate.

Protocol

1. Preparation of the Modified Surfaces

1. Manually polish the test piece (hollow copper cylinder with a 40-mm length (l), a 25-mm outer diameter (d_o), and an 18-mm inner diameter (d_i)) for 15 min using a #2,000 emery paper. Clean the polished surface by rinsing it with acetone followed by DI water.
2. Place the polished test piece in an oven for 2 h at a constant temperature of 120 °C.
3. Prepare a superhydrophilic SiO_2 nanoparticle solution using the following steps.
    1. Prepare solution A by mixing 1:4 molar ratios of tetraethoxy silane and DI water. Add 2 drops of 37% concentrated HCl to solution A and stir for 2 h.
    2. Make solution B by mixing a 1:3 molar ratio of ethanol and DI water.
    3. Mix 1 mL of solution A to 80 mL of solution B and stir for 2 h.
    4. Add 32 g of SiO_2 nanoparticles (40-nm diameter) to the prepared solution and stir for 1 h.
4. Immerse the test piece in the prepared solution by using the dip-coating apparatus at a velocity of 5 mm/min. Keep the coated test piece in an oven at 120 °C for 1 h.
5. Prepare 2, 4, and 8 interlined hybrid patterns with different orientations along the axial direction (as shown in **Figure 1**) using the following steps.
    1. Mask the area to be uncoated using the insulation tape according to the required number of interlines with the proper orientation (For the 2-interline surface at a 0° orientation, adjust interlines at the center and the superhydrophilic area (area to be coated)on the top side. On the other hand, for the 90° orientation, adjust one interline at the top and another at the bottom and for the 180° orientation, adjust superhydrophilic area at the bottom and the interlines at the center. Similarly, adjust the position of the 4, 8 interlined surfaces with the different orientation as shown in **Figure 1**).
    2. Immerse the masked test piece in the prepared solution by using a dip-coating apparatus, dip at a high dipping velocity and rise at a slow velocity of 5 mm/min. Keep the coated test piece in an oven at 120 °C for 1 h.
    3. Remove the insulation tape from the masked area to obtain the required number of interlines with the proper orientation.

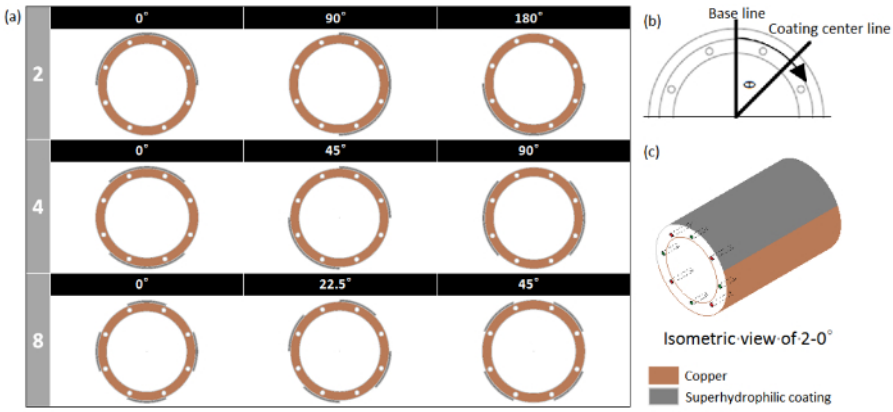

Figure 1. Selection of Various Interlined Surfaces. (a) Schematic of various interlined surfaces with different orientations. The area ratio of a plain copper surface and a superhydrophilic surface is 1:1 in all conditions. **(b)** Orientation selection criteria. **(c)** Isometric view of the 2 interline 0° angle oriented surface. Orientation is selected as the angle between the baseline and coating center line of the first hydrophilic pattern from the top side and it is measured in a clockwise direction. Please click here to view a larger version of this figure.

2. Experimental Procedure

1. Using the insulation tape, fix one glass tube at each circular base of the coated test piece.
2. Horizontally fix this assembly to the 140- x 140- x 160-mm chamber (as shown in **Figure 2**) using silicon paste according the required position of interlines.
3. Place a 550-W, 18-mm diameter, and 40 mm-long cartridge heater with a thin film of thermal paste on the circumferential area into the hole of the test piece.
4. Connect the cartridge heater to a direct current (DC) power supply unit.
5. Place T-type thermocouples into the 8 equally-spaced 1-mm holes, with alternate depths of 5 mm and 7 mm as shown in **Figure 3** Connect them to the data logger.
6. Insert and fix resistance temperature detectors (RTD), a reflux condenser, and an auxiliary heater in the spaces provided on the top cover. Fix them over the boiling chamber.
7. Fill 1,400 mL of DI water into the pool-boiling chamber.
8. Connect the reflux condenser to a cooling chamber that is maintained at 5 °C.
9. Prior to the experiment, vigorously boil the DI water in the pool-boiling chamber for 30 min using the auxiliary heater.

10. Keep the DI water at the saturated boiling condition by using the auxiliary heater. Subsequently, switch on the power supply and give an initial current of 0.1 A.
11. Wait for 2 min in order to reach a steady state. Then, increase the electric current with increments of 0.3 A.
12. Record the temperature at each power input by using the data logger. Continue the experiment until a maximum current of 4 A is reached. Meanwhile, record the bubble dynamics for each power input by using a CCD camera placed in front of the pool-boiling chamber, which is focused on the test piece.

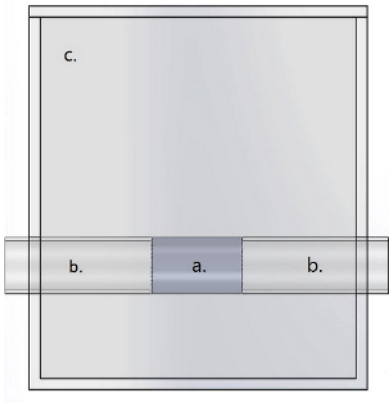

a. Hollow copper cylinder
b. Fixing glass tubes
c. Pool boiling chamber

Figure 2. Schematic of the Pool-boiling Chamber. Glass tubes are connected to both sides of the hollow copper cylinder with silicon paste. This is fixed to the pool-boiling chamber with silicon paste. Please click here to view a larger version of this figure.

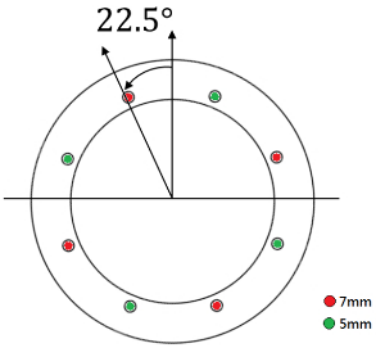

Figure 3. Thermocouple Positioning. 8 thermocouples are placed inside the 1 mm diameter holes circumferentially in the test piece place at a diameter of 20 mm. The depths of alternate 1mm diameter holes are fixed at 5 mm and 7 mm respectively. Please click here to view a larger version of this figure.

3. Data Reduction

1. Calculate the heat input (Q) by using the following equation[19]
   $Q = IV$ (1)
   NOTE: I and *V* are the input current in amps and the voltage in volts, respectively.
2. Estimate the heat loss (Q_{loss}) from the two side surfaces by using the formula[19]:
   $$Q_{loss} = 2\times k\times\left[\frac{(T_{7\ mm}-T_{5\ mm})}{\Delta x}\right]\times A_c \quad (2)$$
   NOTE: k is the thermal conductivity of copper; $T_{7\ mm}$ and $T_{5\ mm}$ are the average values of the temperature at depths of 7 mm and 5 mm, respectively; Δx (2 mm) is the difference between the depths; and
   $A_c = \pi/4(d_o^{\ 2} - d_i^{\ 2})$ is the cross-sectional area of the test piece.
3. Determine the heat flux (q") by using the following formula[19]:
   $$q'' = \frac{Q-Q_{loss}}{A} \quad (3)$$
   NOTE: $A = \pi d_o l$ is the circumferential area of the test piece.
4. Calculate the wall superheat (using the following equation[19]:
   $$\Delta T_w = T_m - \left[\frac{Q-Q_{loss}}{2\pi Lk}\right]\times \ln\left(\frac{r_o}{r_m}\right) - T_{sat} \quad (4)$$

NOTE: T_m is the average of $T_{7\,mm}$ and $T_{5\,mm}$, is the length of the test piece, r_o (12.5 mm) outer radius of the test piece, r_m (10 mm) radius of the test piece at the measuring holes, and T_{sat} is the saturation temperature of DI water as shown in **Figure 4**.

5. Calculate the HTC (α) using the following formula[19]:

$$\alpha = \frac{q''}{\Delta T_w} \quad (5)$$

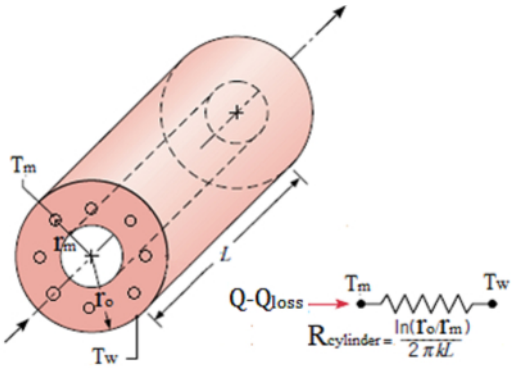

Figure 4. Schematic of Wall Temperature Analysis. Wall temperature is calculated using the measured average temperature and known cylindrical thermal resistance. Please click here to view a larger version of this figure.

Representative Results

Pool-boiling heat-transfer experiments were conducted on a hybrid wettable cylindrical surface using the experimental setup whose schematic is shown in **Figure 5**. The pool-boiling experimental procedure explained in step 2 of the protocol section was successfully carried out while investigating the effect of the number of interlines and of the orientation of the hybrid wettable pattern on the pool-boiling performance. The pool-boiling performances of the different-treated surfaces were represented in terms of graphs: the heat flux versus the wall superheat and the HTC versus the heat flux.

In order to validate the experimental setup, pool boiling experimental heat transfer results of the plain copper surface were compared with the theoretical correlation predicted by Cornwell and Houston in 1994[20], as shown in the following equation:

$$N_u = AF(p)Re_b^{0.67}Pr^{0.4} \quad (6)$$

where N_u is the Nusselt number; $A = 9.7p_c^{0.5}$, with p_c = 221.2 bar; $F(p) = 1.8p_r^{0.17} + 4p_r^{1.2} + 10p_r^{10}$, with $p_r = p/p_c$ and p = 1.013 bar; Re_b is the boiling Reynolds number calculated by using **Equation 7,** and Pr is the Prandtl number.

$$Re_b = \frac{q''\,D}{\mu_f\,h_{fg}} \quad (7)$$

where q" is the heat flux, D is the outer diameter of the test piece, μ_f is the dynamic viscosity, and h_{fg} is the latent heat of vaporization at saturation temperature.
The experimental Nusselt number is calculated by using the following equation:

$$N_u = \alpha D/k_f \quad (8)$$

where α is the HTC and k_f is the thermal conductivity of the working fluid.

Figure 6 shows the validation graph. The experimental Nusselt number is almost the same as the theoretical correlation Nusselt number for a particular Reynolds number.

Experimental uncertainty in the calculated heat flux, the wall super heat and the HTC were calculated using Kline and McClintn method[21]. Uncertainty in heat flux, the wall super heat and the HTC were estimated in the range ±15.3%, ± 1.7%, ± 15.5% respectively.

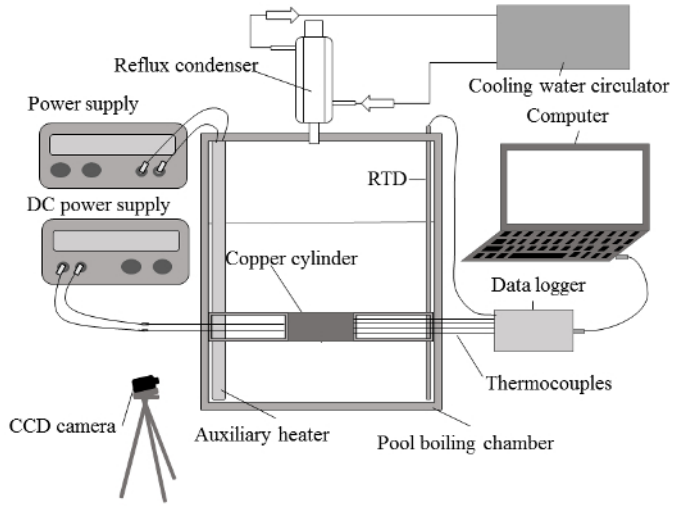

Figure 5. Schematic of the experimental setup. The experimental setup used to investigate the pool-boiling performances. Please click here to view a larger version of this figure.

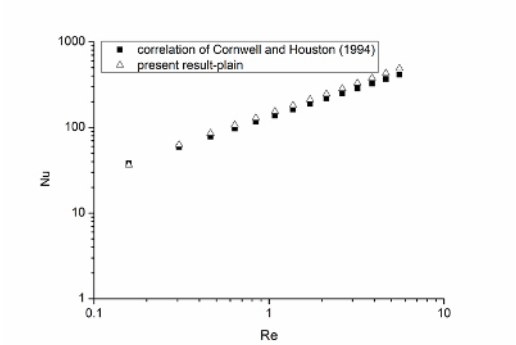

Figure 6. Validation of the experimental setup. A comparison between the present results and the correlation reported by Cornwell and Houston[16] in a logarithmic scale. Please click here to view a larger version of this figure.

Figure 7 (a) shows pool-boiling curves of the plain copper surface, a fully superhydrophilic surface, and hybrid surfaces with different numbers of interlines at a 0° orientation. The pool-boiling curve was obtained by plotting the graph of the heat flux versus the wall superheat. The heat flux and wall superheat were calculated by using **Equations 3** and **4**, respectively. A leftward shift in the pool-boiling curve was obtained for the 8-interline surface, whereas the 2- and 4-interline surfaces showed almost similar values. **Figure 7 (b)** shows the graph of the HTC versus the heat flux of different surfaces. The HTC is calculated by using **Equation 5**. The HTCs of different surfaces were compared, and the 8-interline surface showed the highest value, whereas the homogeneous superhydrophilic surface showed the lowest value.

Bubble nucleation sites of the different surfaces were recorded using a CCD camera. **Figure 8** indicates that the number of bubbles on the fully superhydrophilic surface is the lowest, and with an increase in the number of interlines, the bubbles were also found to increase.

The pool-boiling performance of 2-, 4-, and 8-interlined surfaces and with different orientations are shown in **Figures 9** and **10**. As compared to the pool-boiling curve of the 0° orientation, the 180° orientation showed a rightward shift. In the case of 2-interlined surfaces with different degrees of angular orientation, the 0° orientation showed a better boiling performance. 4- and 8-interlined surfaces gave their maximum enhancement at orientations of 90° and 45°, respectively. In these cases, the positions of the superhydrophilic surfaces were just above the lowermost interlines. **Figure 11** shows the best pool-boiling performances of different interlines. With an increase in interline number, the HTCs are found to improve.

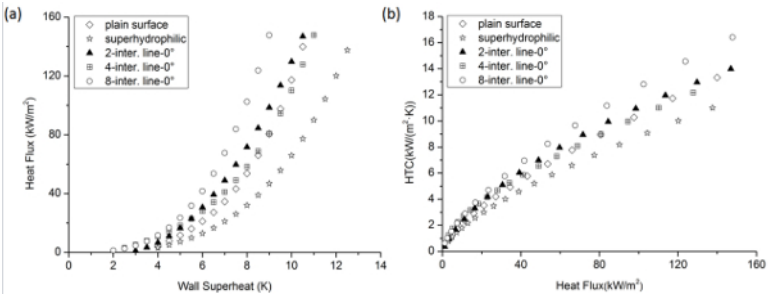

Figure 7. Pool-boiling performance at a 0° orientation. (a) Boiling curves for the various surfaces. **(b)** Graph of the HTC versus the heat flux. Please click here to view a larger version of this figure.

Type of Surface	Surface nucleation
Plain surface	
Superhydrophilic surface	
2-interlaced lines	
4-interlaced lines	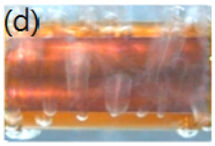
8-interlaced lines	

Figure 8. Photographs of bubble nucleation. (a) Plain surface. **(b)** Superhydrophilic surface. **(c)** 2-interlined surface. **(d)** 4-interlined surface. **(e)** 8-interlined surface. Please click here to view a larger version of this figure.

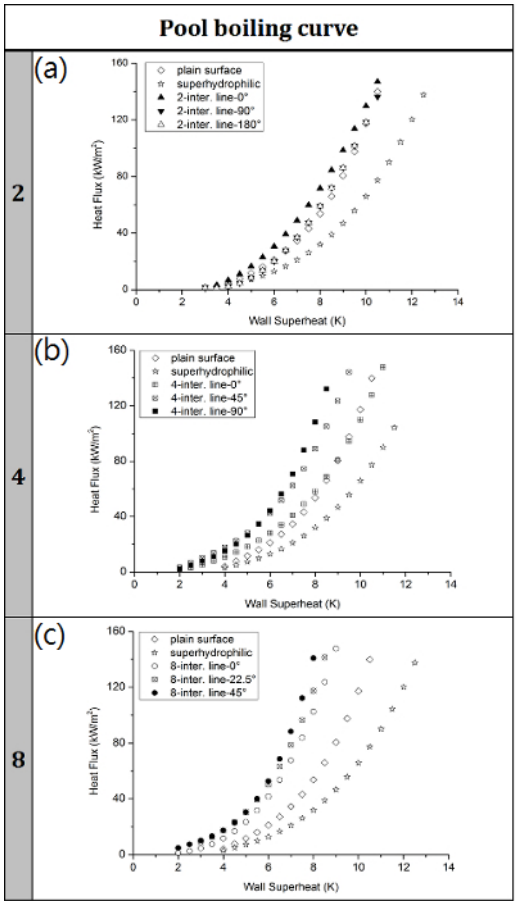

Figure 9. Effect of orientation on the pool-boiling curve. Pool-boiling curves of **(a)** a 2-interlined surface, **(b)** a 4-interlined surface, and **(c)** an 8-interlined surface with different orientations. Please click here to view a larger version of this figure.

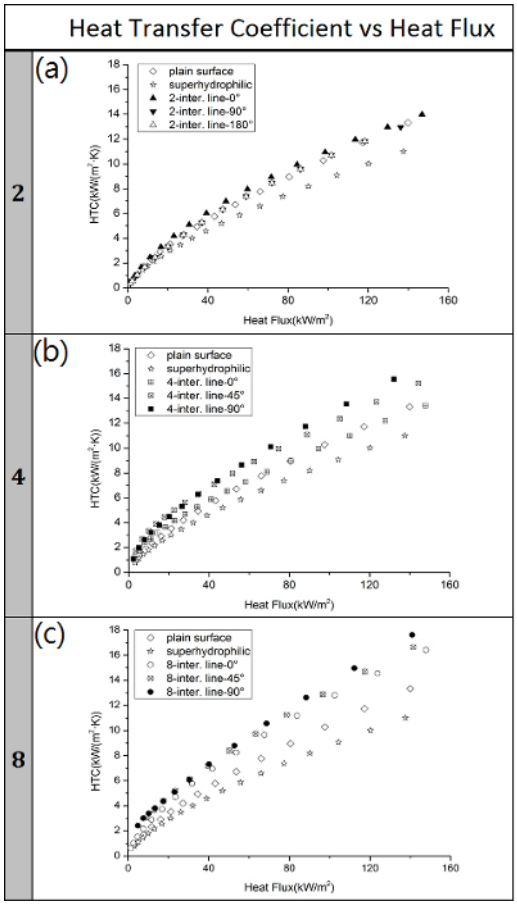

Figure 10. Effect of orientation on the HTC versus the heat flux. The HTC versus the heat flux graph of **(a)** a 2-interlined surface, **(b)** a 4-interlined surface, and **(c)** an 8-interlined surface with different orientations. Please click here to view a larger version of this figure.

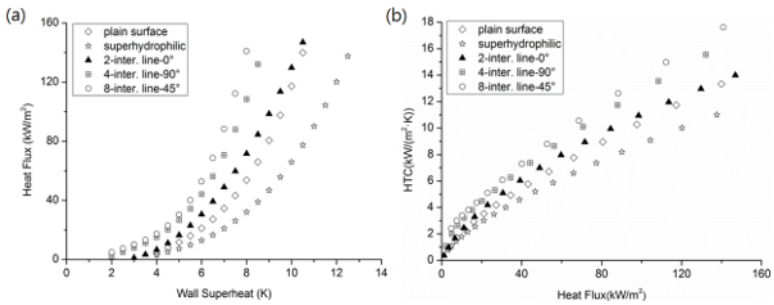

Figure 11. Comparison of the best pool-boiling performances. (a) Boiling curves for the various surfaces. **(b)** Graph of the boiling HTC versus the heat flux. Please click here to view a larger version of this figure.

Discussion

The main goal of this investigation was to develop a pool-boiling heat sink for high heat dissipation applications, such as nuclear reactors, boilers, and heat pipes, by introducing the hybrid wettable surface, as described in the protocol section. These surfaces can produce better pool-boiling performances than homogeneous wettable surfaces (hydrophilic and hydrophobic). The improvement in the boiling heat-transfer performance is due to an increase in active nucleation sites and the easy detachment of the formed bubbles from the surface. In this study, we considered the effects of the number of interlines and the orientation of the hybrid wettable patterns on the pool-boiling performance. The maximum number of interlines was limited to 8 due to the manual preparation method used. The precise positioning of interlines is crucial for all experiments, as a slight misalignment in position will lead to incorrect results. Furthermore, the maximum applied-input current plays a significant role in the life of the cartridge heater. In this study, for safety purposes, the maximum input current is limited to 4 A. Due to this limitation, pool-boiling heat-transfer studies were carried out for only the lower heat flux condition. It is impossible to determine the CHF by using the present experimental setup.

Hybrid wettable patterns play a key role in boiling heat-transfer. The boiling performance of axial interlaced hybrid structures on a cylindrical copper surface depends on the number of interlines and on the orientation of the hybrid wettable pattern. With an increase in the number of interlines, the boiling performance was found to be improved. This is due to the increase in nucleation sites on the interlines. The different hybrid

wettable patterns and the position of the superhydrophilic surface play an important role in boiling heat-transfer. The lowermost interlines with an upper superhydrophilic surface give better heat-transfer performances due to the easy detachment of the formed bubbles from the interlines. During the pool-boiling experiment, the formed bubbles usually try to bend towards the top surface. Because of the low affinity of bubbles to the superhydrophilic surface, they will easily detach from the interlines, which in turn improves the pool-boiling performance.

In conclusion, the pool-boiling performance of the axial interline surfaces depends on both the number of interlines and on the orientation of the hybrid wettable pattern. With an increase in number of interlines, the nucleation sites increase, so the detachment of the formed bubbles from the lowermost interlines with an upper superhydrophilic surface will be fast.

Disclosures

The authors declare that they have no competing financial interests.

Acknowledgements

The authors gratefully acknowledge funding support from the Ministry of Science and Technology, MOST (project numbers: MOST 104-2218-E-002 -004, MOST 105-2218-E-002-019, MOST 105-2221-E-002 -107 -MY3, MOST 102-2221-E-002 -133 -MY3, and MOST 102-2221-E-002 -088 -MY3).

References

1. Putsch, G., Thermal challenges in the next generation of supercomputers. *Proc. CoolCon MEECC Conference,*. 1-83, (2005).
2. Phan, H.T., Caney, N., Marty, P., Colasson, S., & Gavillet, J., Surface wettability control by nanocoating: The effect on pool boiling heat transfer and nucleation mechanism, *Int. J. Heat and Mass Transfer.* **52**, 5459-5471, (2009).
3. J. Barber, D. Brutin, & Tadrist, L., A review on boiling heat transfer enhancement with nanofluids, *Nanoscale Res. Lett.* **6**, 280, (2011).
4. Kim, S.J., Bang, I.C., Buongiorno, J., & Hu, L. W., Effects of nanoparticle deposition on surface wettability influencing boiling heat transfer in nanofluids, *Appl. Phys. Lett.* **89**, 153107, (2006).
5. Berenson, P.J., Experiments on pool-boiling heat transfer, *Int. J. Heat Mass Transfer.* **5** (10), 985-999, (1962).
6. You, S.M, Simon, T. W, & Bar-Cohen, A., A technique for enhancing boiling heat transfer with application to cooling of electronic equipment, *IEEE Trans. Compon. Hybrids Manuf. Tech.* **15** (5), 823-831, (1992).
7. Li, C., & Peterson, G.P., Parametric study of pool boiling on horizontal highly conductive microporous coated surfaces, *J. Heat Transfer.* **129** (11), 1465-1475, (2007).
8. Trisaksri,V., & Wongwises, S., Critical review of heat transfer characteristics of nanofluids. *Renew. Sust. Energy Rev.* **11** (3), 512-523, (2007).
9. Trisaksri,V., & Wongwises, S., Nucleate Pool Boiling Heat Transfer of TiO_2-R141b nanofluids, *Int. J. Heat Mass Transfer.* **52** (5-6), 1582-1588, (2009).
10. Suriyawong, A, & Wongwises, S., Nucleate pool boiling heat transfer characteristics of TiO_2- water nanofluids at very low concentrations, *Exp. Therm. Fluid Sci.* **34** (8), 992-999, (2010).
11. Suriyawong, A., Dalkilic, A. S., & Wongwises, S., Nucleate Pool Boiling Heat Transfer Correlation for TiO2-Water Nanofluids, *J. ASTM Int.* **9** (5), 1-12, (2012).
12. Sarangi, S., Weibel, J.A., & Garimella, S.V., Effect of particle size on surface-coating enhancement of pool boiling heat transfer, *Int. J. Heat Mass Transfer.* **81,** 103-113, (2015).
13. Kumar, C.S.S., Suresh, S., Kumar, M.C.S., & Gopi, V., Effect of surfactant addition on hydrophilicity of ZnO-Al2O3 composite and enhancement of flow boiling heat transfer, *Exp. Therm. Fluid Sci.* **70**, 325-334, (2016).
14. Takata, Y., Hidaka, S., & Uraguchi, T., Boiling feature on a super water-repellent surface, *Heat Transfer Eng.* **27** (8), 25-30, (2006).
15. Takata, Y., Hidaka, S., Masuda, M., & Ito, T., Pool boiling on a super hydrophilic surface, *Int. J. Energy Res.* **27**, 111-119, (2003).
16. Takata, Y., Hidaka, S., & Kohno, M., Enhanced nucleate boiling by super hydrophobic coating with checkered and spotted patterns, *International Conference on Boiling Heat Transfer.*, Spoleto, (2006).
17. Hsu, C.C., Chiu, W. C., Kuo, L. S., & Chen, P.H, Reversed boiling curve phenomenon on surfaces with interlaced wettability, *AIP Advances.* **4** 107110, (2014).
18. Jo, H., Ahn, H. S., Kang, S.H., & Kim, M. H., A study of nucleate boiling heat transfer on hydrophilic, hydrophobic and heterogeneous wetting surface, *Int. J. Heat Mass Transfer.* **54**, 5643-5652, (2011).
19. Mehta, J.S., & Kandlikar, S.G., Pool boiling heat transfer enhancement over cylindrical tubes with water at atmospheric pressure, Part I: Experimental results for circumferential rectangular open microchannels, *Int. J. Heat Mass Transfer.* **64**, 1205-1215, (2013).
20. Cornwell, K., & Houston, S.D., Nucleate Pool Boiling on Horizontal Tubes - a Convection-Based Correlation, *Int. J. Heat Mass Transfer.* **37**, 303-309, (1994).
21. Holman, J.P. *Experimental Methods for Engineers.*,(seventh ed.)Tata McGraw Hill Education Private Limited (2007).

